Published in final edited form as:
Immunity. 2013 May 23; 38(5): 906–917. doi:10.1016/j.immuni.2013.04.007.

A truncated splice-variant of the FcεRIβ receptor subunit is critical for microtubule formation and degranulation in mast cells

Glenn Cruse[1,*], **Michael A. Beaven**[2], **Ian Ashmole**[3], **Peter Bradding**[3], **Alasdair M. Gilfillan**[1], and **Dean D. Metcalfe**[1]

[1]Laboratory of Allergic Diseases, National Institute of Allergy and Infectious Diseases, National Institutes of Health, Bethesda, MD 20892, USA

[2]Laboratory of Molecular Immunology, National Heart, Lung and Blood Institute, National Institutes of Health, Bethesda, MD 20892, USA

[3]Department of Infection, Immunity and Inflammation, Institute for Lung Health, University of Leicester, Glenfield Hospital, Leicester, LE3 9QP, UK

Summary

Human linkage analyses have implicated the *MS4A2*-containing gene locus (encoding FcεRIβ) as a candidate for allergy susceptibility. We have identified a truncation of FcεRIβ (t-FcεRIβ) in humans which contains a putative calmodulin binding domain and thus, we sought to identify the role of this variant in mast cell function. We determined that t-FcεRIβ is critical for microtubule formation and degranulation and that it may perform this function by trafficking adapter molecules and kinases to the pericentrosomal and Golgi region in response to Ca^{2+} signals. Mutagenesis studies suggest that calmodulin binding to t-FcεRIβ in the presence of Ca^{2+} could be critical for t-FcεRIβ function. In addition, gene targeting of t-FcεRIβ attenuated microtubule formation, degranulation and IL-8 production downstream of Ca^{2+} signals. Therefore, t-FcεRIβ mediates Ca^{2+}-dependent microtubule formation, which promotes degranulation and cytokine release. Because t-FcεRIβ has this critical function, it represents a therapeutic target for the down-regulation of allergic inflammation.

Introduction

Aggregation of high affinity receptors for IgE (FcεRI) by multivalent Ag initiates mast cell (MC) activation and release of chemical mediators that initiate allergic inflammation (reviewed in (Gilfillan and Rivera, 2009; Gilfillan and Tkaczyk, 2006; Rivera and Gilfillan, 2006)). The FcεRI, expressed on MC, exists as a tetrameric receptor complex comprised of an IgE-binding α chain with a single transmembrane domain, a tetra-transmembrane-spanning β chain (encoded by the *MS4A2* gene) and a disulphide-linked homodimer of signal-transducing γ chains (Kinet, 1999). The FcεRIα subunit binds IgE with high affinity, but FcεRI signaling is mediated by immunoreceptor tyrosine-based activation motifs

*Correspondence: glenncruse@hotmail.com.

The authors declare no conflicts of interest.

(ITAM)s in the cytoplasmic domains of the FcεRIγ subunits. These recruit and activate Syk kinase initiating the signaling cascade (Gilfillan and Rivera, 2009; Gilfillan and Tkaczyk, 2006; Rivera and Gilfillan, 2006). The FcεRIβ subunit also has signaling capabilities, imparted through its non-canonical ITAM near the C-terminus. Upon phosphorylation, the FcεRIβ ITAM binds Lyn kinase leading to the recruitment and phosphorylation of Syk kinase, thus amplifying FcεRIγ-mediated signaling (Gilfillan and Tkaczyk, 2006; Lin et al., 1996; Rivera and Gilfillan, 2006). In mice, FcεRIβ also amplifies FcεRI signaling by promoting the assembly, stabilization and trafficking of the receptor complex to the cell surface (Donnadieu et al., 2000b; Ra et al., 1989; Singleton et al., 2009).

The gene locus containing *MS4A2* has strong linkage to allergy susceptibility (Cookson et al., 1989; Laprise et al., 2000; Sandford et al., 1993). Given the known functions of FcεRIβ, *MS4A2* was thus considered as a candidate gene for the development of allergy and asthma (Sandford et al., 1993; Shirakawa et al., 1994). However, studies investigating the functional consequence of the asthma-associated mutations in *MS4A2* were disappointing because transfection of the mutant forms showed no effect on FcεRIβ function (Donnadieu et al., 2000a). More recently, mutations in the predicted transcription promoter region for *MS4A2* have been identified (Kim et al., 2006; Nishiyama et al., 2004) but the implications of these findings are not yet clear.

We recently identified a truncated splice variant of FcεRIβ (t-FcεRIβ) (GenBank: JF411082.1) in human (Hu)MC which lacks exon 3, leading to loss of the first 2 transmembrane domains (Cruse et al., 2010) that are required for binding to FcεRIα and receptor trafficking (Singleton et al., 2009). As a result, this variant does not traffic to the plasma membrane but has a more diffuse distribution with evidence of nuclear membrane and peri-nuclear localization (Cruse et al., 2010). Whether t-FcεRIβ plays a role in Ag-mediated MC activation is unknown but, because t-FcεRIβ retains the C-terminal ITAM, (Cruse et al., 2010) we have examined the hypothesis that t-FcεRIβ retains signaling capability. Based on an examination of the comparative roles of FcεRIβ and t-FcεRIβ splice variants in HuMC signaling, we present data which support the conclusion that t-FcεRIβ propagates Ca^{2+} signals which initiate microtubule formation and thereby promote mediator release. Therefore, we demonstrate that t-FcεRIβ plays an important role in mast cell degranulation and could thus contribute to the allergic response.

Results

Validation of shRNA targeting of FcεRIβ variants

The two variants of FcεRIβ expressed in HuMC, full length (FL)-FcεRIβ - *MS4A2* (NM_000139.4) and t-FcεRIβ - $MS4A2_{trunc}$ (JF411082.1) (Figure S1A and B) - were analyzed independently by targeting the exon 2 – exon 3 boundary as we described (Cruse et al., 2010). T-FcεRIβ lacks exon 3 and can be identified independently of FL-FcεRIβ (Figure S1A). The functions of the protein products were explored following shRNA-mediated FcεRIβ silencing. The efficacy of 3 shRNA constructs (MS4A2v1, MS4A2v2 and MS4A2v3) to reduce FcεRIβ expression were initially examined. shMS4A2v1 targets exon 7 of FcεRIβ, whilst shMS4A2v2 targets exon 3 so should not affect t-FcεRIβ expression as this lacks exon 3. shMS4A2v3 targets the exon 1–2 boundary (Figure S1A).

All shRNA constructs reduced FL-FcεRIβ mRNA expression to some degree at day 7 post infection. The most effective construct was shMS4A2v3 which silenced both variants of FcεRIβ with equal efficacy. shMS4A2v1 silenced both variants, but with lower efficacy than shMS4A2v3. Importantly, shMS4A2v2 effectively silenced FL-FcεRIβ while having minimal impact on t-FcεRIβ expression (Figure 1A). Thus, to examine the relative role(s) of

t-FcεRIβ and FcεRIβ in MC function we compared the differential abilities of shMS4A2v2 and shMS4A2v3 to modulate defined responses in LAD-2 HuMC in subsequent studies.

We next confirmed that silencing of mRNA resulted in reduction of FcεRIβ protein expression. We observed that 2 proteins of ~22 kDa and ~28 kDa were expressed in WT mouse bone marrow-derived MC (mBMMC) and the LAD-2 HuMC line (Figure 1B), but were absent in *Ms4a2*$^{-/-}$ mBMMC. At 7 days post infection, FL-FcεRIβ protein expression with silencing was reduced (Figures 1B and S1C). There was excellent correlation between the degree of mRNA and protein reduction of FL-FcεRIβ with the different shRNA constructs (Figure 1C). FcεRIβ silencing in mBMMC reduced expression of both variants. In the LAD-2 HuMC, shMS4A2v2 preferentially silenced FL-FcεRIβ over t-FcεRIβ and shMS4A2v3 silenced both variants (Figure 1B). Taken together, these data indicate that FcεRIβ isoforms can be differentially silenced using the shRNA constructs tested.

FcεRIβ gene-targeting reduces FcεRIα surface expression without affecting KIT expression

Because FcεRIβ is required for FcεRI surface expression in the mouse, and may facilitate FcεRI expression in humans (Donnadieu et al 2000a), we examined the effects of FcεRIβ silencing on the surface expression of both FcεRIα and KIT in LAD-2 HuMC. Silencing of FL-FcεRIβ (shMS4A2v2) and simultaneous silencing of both FcεRIβ variants (shMS4A2v3) had no substantial effect on KIT expression either at the cell surface or within permeabilized cells (Figure 1D). However, as expected, both constructs reduced the expression of FcεRIα at the cell surface (Figures 1D and S1D). Permeabilization of the cells did not substantially change the degree of FcεRIα staining (Figure 1D). The degree of FL-FcεRIβ protein expression with silencing closely matched the amount of surface FcεRIα expression (Figure S1E). There was no difference between silencing of FL-FcεRIβ and silencing of both FcεRIβ variants except that the shMS4A2v3 construct that silences both FcεRIβ variants was more effective at reducing surface FcεRIα expression. These data confirm that FcεRIβ is required for surface expression of FcεRI.

Different roles for FcεRIβ variants in Ag/IgE-dependent and Ag/IgE-independent degranulation

Because FcεRI expression was reduced with silencing of both FL-FcεRIβ and t-FcεRIβ variants, we examined the manifestations of FcεRIβ silencing on MC degranulation as assessed by β-hexosaminidase (β-hex) release. Targeting just FL-FcεRIβ (shMS4A2v2) and concurrent silencing of both FcεRIβ variants (shMS4A2v3) markedly inhibited Ag-induced degranulation in LAD-2 HuMC (Figure 2A). The addition of SCF when challenging MC with Ag potentiates Ag-dependent degranulation (Hundley et al., 2004), but we found that adding SCF did not change the degree of inhibition observed with either shRNA construct (Figure 2B). There was a strong correlation between the amount of degranulation with each shRNA construct, FcεRIβ expression (Figure S2A) and surface FcεRIα expression (Figure S2B), supporting the conclusion that inhibition of IgE-dependent degranulation with the FcεRIβ silencing was due to a reduction in FcεRI expression.

As both shRNA constructs exhibited reduced degranulation with Ag stimulation, we examined responses to IgE-independent stimulation. LAD-2 HuMC degranulate in response to the anaphylatoxin C3a, which acts *via* the G protein-coupled receptor C3aR (Kashem et al., 2011). In contrast to FcεRI-mediated degranulation, C3a-induced LAD-2 HuMC degranulation was potentiated with shMS4A2v2 silencing of FL-FcεRIβ. However, the additional targeting of the t-FcεRIβ variant with shMS4A2v3 impaired degranulation induced by C3a (Figure 2C). We also examined the effects of FcεRIβ silencing on degranulation in response to thapsigargin. Thapsigargin stimulates MC degranulation

through a receptor-independent mechanism by depleting endoplasmic reticular Ca^{2+} stores (Thastrup et al., 1990) initiating store-operated Ca^{2+} entry through the Ca^{2+} channel protein Orai1 (Ma and Beaven, 2011). There was no difference in the degree of degranulation induced by high concentrations of thapsigargin (>100 nM) when comparing the scramble control cells to shMS4A2v2 silencing of FL-FcεRIβ, but with sub-maximal concentrations of thapsigargin (10 nM) degranulation was enhanced. In contrast, thapsigargin-induced degranulation at all concentrations was reduced in cells where t-FcεRIβ was additionally silenced with shMS4A2v3 (Figure 2D). Thus, the inhibition of degranulation following silencing of t-FcεRIβ appeared to be downstream of processes that regulate the Ca^{2+} signal. Also, the differential effects of shMS4A2v2 and shMS4A2v3 on LAD-2 HuMC IgE-independent degranulation supported our supposition that comparative studies with both constructs could adequately unmask the functional consequences of t-FcεRIβ depletion even though t-FcεRIβ itself could not be selectively silenced.

The potentiation of IgE-independent degranulation following silencing of FL-FcεRIβ suggests that FcεRIβ may have an inhibitory role in this circumstance. To test this further, we overexpressed FL-FcεRIβ and t-FcεRIβ in LAD-2 HuMC and tested the effects on degranulation in response to both Ag and thapsigargin. We found that overexpression of FL-FcεRIβ reduced degranulation, whilst overexpression of t-FcεRIβ potentiated degranulation with both Ag (Figure 2E) and thapsigargin (Figure 2F). To determine if this was also true in non-transformed HuMC, we overexpressed FL-FcεRIβ in human lung MC (HLMC) as described (Cruse et al., 2010), then activated the cells with anti-IgE. Under these conditions, histamine release was also attenuated compared to control cells (Figure S2C). This supports previous studies which show that whilst FL-FcεRIβ is required for surface expression of FcεRI, it can also inhibit degranulation (Furumoto et al., 2004; Gimborn et al., 2005). Conversely, overexpression of t-FcεRIβ potentiated degranulation in LAD-2 HuMC (Figure S2D). In addition, silencing of both FcεRIβ variants in HLMC attenuated degranulation in response to both anti-FcεRI and thapsigargin (Figure S2E). These studies collectively demonstrate differential roles for FcεRIβ isoforms in both IgE-dependent and -independent degranulation.

Targeting of t-FcεRIβ inhibits production of IL-8 but not PGD_2

Because FcεRIβ isoforms have differing roles in the induction of HuMC degranulation, we conducted similar studies on the *de novo* generation of PGD_2. Ag-induced PGD_2 synthesis was impaired with silencing of FL-FcεRIβ or both FcεRIβ variants (Figure 2G). C3a did not induce significant release of PGD_2 in any of these conditions (Figure 2H). However, in marked contrast to degranulation, there were no significant differences between either of the shRNA constructs and the scramble control (Figure 2I). Due to the discordance between degranulation and PGD_2 generation upon thapsigargin stimulation, we next examined IL-8 production. We were unable to detect IL-8 release with Ag or C3a stimulation in the LAD-2 HuMC (data not shown). However, IL-8 production in response to thapsigargin stimulation was potentiated with silencing of FL-FcεRIβ with shMS4A2v2 when compared to control, whereas additional silencing of t-FcεRIβ with shMS4A2v3 inhibited thapsigargin-induced IL-8 release (Figure 2J). These data are consistent with the conclusion that silencing of the t-FcεRIβ variant inhibits degranulation and the release of IL-8 but not PGD_2 production.

Effect of targeting FcεRIβ and t-FcεRIβ on Ca^{2+} signaling

We next examined whether the effects of silencing FcεRIβ variants on Ca^{2+} signals. There was a significant reduction in the ability of Ag to increase intracellular Ca^{2+} either in the absence (Figure 2K) or presence of 100 ng/ml SCF (Figure 2L) with silencing of FL-FcεRIβ or both variants of FcεRIβ. However, this reduction was greater with silencing of both FcεRIβ variants with shMS4A2v3. These data may reflect the larger reduction in FcεRIα

surface expression and Ag sensitivity with shMS4A2v3 over shMS4A2v2 (as in Figure S1). Release of Ca^{2+} from intracellular stores was unaffected by gene-silencing (Figure 2M). However, induction of Ca^{2+} influx with thapsigargin was reduced when FL-FcεRIβ was silenced and a more marked reduction in Ca^{2+} influx was evident with silencing of both FcεRIβ variants (Figure 2M). Although Ca^{2+} influx was impaired with silencing of both FcεRIβ variants when compared to controls, the relatively small effect on Ca^{2+} would be insufficient for the degree of inhibition of degranulation, suggesting that the mechanism of inhibition of degranulation and IL-8 production following gene-silencing of both FcεRIβ variants was not primarily due to defective Ca^{2+} signaling but rather to impediments in downstream or Ca^{2+}-independent signaling events.

Silencing t-FcεRIβ does not suppress IgE-independent early mast cell signaling events

Given the profound effects on degranulation, we tested whether FcεRI-dependent signaling events such as phosphorylation of phospholipase $C\gamma_1$ ($PLC\gamma_1$), Akt (a surrogate marker for phosphatidylinositol-3-kinase [PI3K] activation), and mitogen-activated protein kinases (MAPK) are similarly compromised with silencing of FcεRIβ in LAD-2 HuMC. The data revealed a reduction in $PLC\gamma_1$ phosphorylation with targeting of FL-FcεRIβ and with silencing of both variants of FcεRIβ when stimulated with Ag (Figures 3A and S3A). There was also a reduction in Ag-induced Akt phosphorylation particularly with silencing of both FcεRIβ variants (Figures 3A and S3B). The effects of silencing FcεRIβ on FcεRI-dependent signaling were also evident at the MAPK level with a reduction in phosphorylation of c-Jun N-terminal kinases (JNK) (Figure S3C) and extracellular signal-related kinases 1/2 (ERK1/2) (Figure S3D), particularly when both variants were silenced (Figure 3A). Importantly, IgE-independent signaling initiated by either C3a or SCF remained intact at all levels although there was a reduction in SCF-induced $PLC\gamma_1$ phosphorylation (Figures 3A and S3A). We also examined the FcεRIβ-dependent phosphorylation of SH2 containing inositol phosphatase (SHIP)-1 which negatively regulates MC signaling and cytokine production (Furumoto et al., 2004). However, there was no significant reduction in SHIP-1 phosphorylation (Y^{1020}) with silencing of either FL-FcεRIβ alone or both variants of FcεRIβ when compared to scrambled control (Figures 3A and S3E).

Earlier we attributed the marked reduction in FcεRI-independent thapsigargin-induced degranulation following silencing of both variants of FcεRIβ to reduced expression of t-FcεRIβ. Thus, we examined the effects of silencing on thapsigargin-induced signaling. Thapsigargin did not induce phosphorylation of Akt kinase or $PLC\gamma_1$ (data not shown). However, phosphorylation of the MAPK's ERK1 and ERK2, JNK and p38 was apparent (Figure 3B compared to unstimulated in Figure 3A) and indeed were potentiated when FL-FcεRIβ was silenced (Figure 3B). Nevertheless, simultaneous silencing of both FcεRIβ variants had no effect on MAPK phosphorylation and silencing of either FL-FcεRIβ or both variants did not affect SHIP1 phosphorylation (Figure 3B). Taken together, the signaling data demonstrate a reduction in Ag-induced signaling, but no reduction in IgE-independent signaling with gene-targeting. This suggests that any defects in signaling that could not be accounted for by a reduction in FcεRI expression were minimal.

T-FcεRIβ co-immunoprecipitates with Gab2, Fyn and calmodulin

Since the defect in MC degranulation was attributed to t-FcεRIβ silencing but appeared to be independent of the early signaling events including Ca^{2+} mobilization, we also examined the sequence of t-FcεRIβ for domains that could bind Ca^{2+}-sensing proteins (Figure S4A and B). Calmodulin (CaM) is a Ca^{2+} binding protein that changes conformation when bound to Ca^{2+} and is essential for Ca^{2+}-mediated MC degranulation (Funaba et al., 2003). Using the Calmodulin Target Database prediction tool (http://calcium.uhnres.utoronto.ca/ctdb/ctdb/

sequence.html), we determined that both variants of FcεRIβ contained a putative CaM binding site (Figure S4A–D). However, this region would be obscured by the plasma membrane in the FL-FcεRIβ (Figure S4C). Conversely, the truncation of FcεRIβ, which results in the loss of the first 2 transmembrane domains, exposes this region for binding CaM (Figure S4D). The potential CaM binding site and adjacent putative *N*myristoylation site, in particular, are highly conserved in human and mouse t-FcεRIβ suggesting a functional significance for these domains (Figure S4E). Therefore, we examined the ability of t-FcεRIβ to bind CaM by probing LAD-2 HuMC lysates with a GFP:t-FcεRIβ chimeric protein. We found that chimeric GFP:t-FcεRIβ pulled down CaM when added to the LAD-2 HuMC lysates, whilst pull-down with GFP itself did not (Figure 4A and B). In addition, CaM pull-down was markedly increased in the presence of Ca^{2+} (Figure 4A). We also probed the co-immunoprecipitates for phosphorylated tyrosine residues and found that there was phosphorylation of proteins corresponding to about 95 kDa, 55 kDa, 45 kDa and 40 kDa only when Ca^{2+} was added (Figure 4A).

From the pull-down data and the functional data, we hypothesized that t-FcεRIβ was sensing Ca^{2+} influx and initiating degranulation. One of the major components of MC degranulation downstream of Ca^{2+} influx is cytoskeletal rearrangement (Blank and Rivera, 2004), a process that is dependent upon the Fyn kinase/Gab2/PI3K pathway (Liu et al., 2007; Nishida et al., 2005; Suzuki et al., 2010). Since Fyn kinase (59 kDa) and Gab2 (97 kDa) correspond to the sizes of bands seen in the pulldowns, we probed for these proteins and found that they too were pulled down in the presence and absence of Ca^{2+} (Figure 4B). We also probed for the binding partner of Gab2, the PI3K p85 subunit, and found that p85 also co-immunoprecipitated with t-FcεRIβ (Figure 4B). Since the Fyn/Gab2/PI3K pathway appears to regulate microtubule formation (Liu et al., 2007; Nishida et al., 2005), and they appear to interact with t-FcεRIβ, we probed for α-tubulin and found that there was a band in the t-FcεRIβ pull-downs, suggesting a direct interaction between the t-FcεRIβ complex and microtubules. There was also a band of 45 kDa which was phosphorylated when Ca^{2+} was added which corresponds exactly to the size of the GFP:t-FcεRIβ chimera suggesting that the ITAM domain of t-FcεRIβ could be phosphorylated upon binding of CaM (Figure 4A pulldown). Although Lyn kinase has also been shown to complex to FcεRIβ (Vonakis et al., 1997), we found only a faint band on probing for Lyn suggesting that the t-FcεRIβ complex preferentially binds Fyn (as in Figure 4B) over Lyn (Figure S4F). Another Src family kinase, Hck, which has been shown to be important in MC degranulation (Hong et al., 2007) was also tested but found not to form part of the t-FcεRIβ complex (Figure S4F).

To study whether CaM was binding to the putative CaM binding domain of t-FcεRIβ, we generated CaM binding domain mutants of t-FcεRIβ. We exchanged polar R residues with non-polar A residues as described in the supplemental methods (CaM mut 1). A random mutation occurred in 1 clone which resulted in an additional Y to D mutation (CaM mut 2) (see supplemental methods). To test the ability of these mutants to bind CaM, we employed the same methodology as in figure 4A and B, and also used a CaM sepharose 4B column to pull-down CaM binding proteins. Using both methodologies, we identified a reduction in CaM binding which was more marked with t-FcεRIβ CaM mut 2 (Figure 4C). We tested the functional consequence of mutation and found that hindering CaM binding to t-FcεRIβ eliminated the potentiation of degranulation seen with WT t-FcεRIβ (Figure 4D and E), suggesting that binding of CaM was critical for t-FcεRIβ function in degranulation. Furthermore, transfection of WT t-FcεRIβ into LAD-2 HuMC partially recovered thapsigargin-induced degranulation after silencing of both FcεRIβ variants, but transfection of t-FcεRIβ CaM mut 2 did not (Figure 4F). This was more evident when degranulation was determined by a LAMP2 assay which was gated on the GFP-positive population (Figure 4G). Taken together, the findings suggest that the function of t-FcεRIβ in degranulation could be dependent upon CaM binding to the putative CaM binding domain of t-FcεRIβ.

Targeting of t-FcεRIβ results in defective microtubule formation and F-actin dynamics

Because t-FcεRIβ interacts with Gab2, PI3K and Fyn kinase we hypothesized that the defect in degranulation upon silencing of t-FcεRIβ was due to defective cytoskeletal rearrangement. Therefore we examined both α-tubulin and F-actin dynamics using confocal microscopy in thapsigargin-stimulated LAD-2 HuMC to bypass effects of FcεRIβ silencing on surface FcεRIα expression and Ag activation. In control cells, there was a decrease in F-actin intensity at 2 min representing depolymerization of cortical F-actin. At 5 and 10 min the intensity markedly increased representing repolymerization (Figures 5A and S5A). Targeting of FL-FcεRIβ had no effect on F-actin depolymerization, although F-actin depolymerization was less evident, and the subsequent increase in intensity was still marked (Figures 5A and S5A). However, with the additional silencing of t-FcεRIβ with shMS4A2v3, actin repolymerization was delayed (Figures 5A and S5A). In mBMMC, we also observed marked depolymerization of F-actin in response to thapsigargin challenge. However, repolymerization was not evident by 10 min in mBMMC, demonstrating different dynamics, and potentially different roles for actin in human and mouse MC degranulation in response to thapsigargin (Figure S5B and C). It was only possible to silence both FcεRIβ variants in the mouse with available constructs, and there were no differences in actin dynamics between the scrambled control and the shMs4a2 constructs in the mBMMC (Figure S5B).

The most palpable defect in cytoskeletal dynamics with silencing of both FcεRIβ variants was α-tubulin assembly into microtubules (Figures 5B and S5D). In control cells and with silencing of FL-FcεRIβ, there was obvious formation of microtubules with the characteristic focal point at the MicroTubule Organization Center (MTOC). The kinetics of microtubule formation appeared to be faster with silencing of FL-FcεRIβ when compared to control cells (Figure S5D). However, most notable was the impairment of microtubule formation when t-FcεRIβ was silenced along with FL-FcεRIβ with shMS4A2v3 (Figures 5B and S5D). This failure could thus account for the reduction in degranulation (Figure 2A). Silencing of both FcεRIβ variants in mBMMC also resulted in defective microtubule formation suggesting a conserved function for t-FcεRIβ in human and mouse MC (Figure S5E and F). In addition, silencing of both FcεRIβ variants in mBMMC resulted in reduced degranulation in response to thapsigargin which correlated well with t-FcεRIβ expression (Figure S5G). These data suggest that t-FcεRIβ plays a role in the regulation of microtubule formation and degranulation in response thapsigargin.

The t-FcεRIβ complex translocates to the Golgi after stimulation

Our data prompted us to examine the intracellular trafficking of t-FcεRIβ. We found that when the GFP:t-FcεRIβ chimera was transfected into LAD-2 HuMC, t-FcεRIβ expression was distributed throughout the cell but most abundantly near the centrosome under resting conditions. However, following stimulation with thapsigargin, t-FcεRIβ transiently translocated to a region adjacent to the nucleus, which was rich in α-tubulin (Movie S1), forming a circular structure around the centrosome (Figure 6A). We stained for Fyn kinase and Gab2 in control and thapsigargin-stimulated cells and found that they also accumulated in the perinuclear region which was more apparent with stimulation (Figure 6B). This localization was less evident in cells where both FcεRIβ variants were silenced (Figure 6B). Stimulation of LAD-2 HuMC with Ag resulted in similar localization of t-FcεRIβ to the MTOC region (Figure S6A). Ag stimulation triggered recruitment of Gab2 to the plasma membrane as well as the MTOC (Figure S6B). However, plasma membrane recruitment of Gab2 with thapsigargin stimulation was less evident (Figure S6C).

To explore t-FcεRIβ localization further, the GFP:t-FcεRIβ chimera constructs were transfected into LAD-2 HuMC and images were acquired by confocal microscopy. Gab2

and t-FcεRIβ were observed to colocalize and form a network concentrated around the MTOC (Figure 7A and B and Figure S7) (Movies S2 and S3) and centrosome (Figure 7C and D) (Movies S4 and S5). This colocalization was less evident with the CaM mut 2 construct (Figures 7A and B and Figure S7) suggesting an important role for the putative CaM binding domain in translocation of t-FcεRIβ. It has been demonstrated that the Golgi Apparatus is usually in close proximity to the MTOC (Hurtado et al., 2011; Rivero et al., 2009) and that the Golgi protein GM130 may play a role in microtubule formation (Hurtado et al., 2011; Rivero et al., 2009). We therefore stained for GM130 and found that t-FcεRIβ colocalized with GM130 (Figure 7E), demonstrating that the t-FcεRIβ complex translocated to the Golgi following stimulation. Thus the localization of the t-FcεRIβ-Gab2 complex to the Golgi appears to be critical for the formation of microtubules and degranulation of HuMC.

Discussion

This study demonstrates multiple roles for the *MS4A2* gene that encodes FcεRIβ in HuMC function. Principally, we demonstrate a crucial role for t-FcεRIβ in that this variant translocates to the Golgi following activation. Importantly, the translocation of t-FcεRIβ may be associated with binding of Ca^{2+}-loaded CaM to t-FcεRIβ. This binding may facilitate phosphorylation of substrates corresponding to Fyn kinase, Gab2 and t-FcεRIβ. Whilst the thesis of such a t-FcεRIβ complex is in agreement with a previous report that Gab2 complexes with Fyn and PI3K (Parravicini et al., 2002), our data cannot rule out independent and/or competitive binding to t-FcεRIβ by kinases. However, mutation of the CaM binding domain of t-FcεRIβ, which results in reduction in CaM pulldown, appears to render t-FcεRIβ non-functional. Thus, we believe that these observations support the construct that phosphorylation of Fyn kinase and Gab2 facilitates translocation of the t-FcεRIβ complex to the Golgi where it plays a role in microtubule formation in a CaM-dependent manner promoting degranulation.

MC signaling has been extensively studied and the FcεRI-proximal pathways involved in MC activation are largely well defined (Reviewed in (Gilfillan and Rivera, 2009; Gilfillan and Tkaczyk, 2006; Rivera and Gilfillan, 2006)). However, signaling events downstream of Ca^{2+} influx are less well studied, but we know that these events involve cytoskeletal dynamics regulating secretory granule trafficking and fusion with the plasma membrane (Draber et al., 2012; Lorentz et al., 2012). It has been demonstrated that in addition to the requirement for Ca^{2+} influx, the Fyn kinase/Gab2/PI3K pathway is critical for the formation of microtubules and hence the trafficking of MC granules to the cell surface (Nishida et al., 2011; Nishida et al., 2005). Our studies provide additional details of the molecular events that may link these critical processes and provide a plausible mechanism for the propagation of Ca^{2+} signals to the cytoskeleton, thus linking Ca^{2+} influx to formation of microtubules and degranulation. An interesting observation particularly pertinent to our suggested model is that events controlling FcεRI-dependent signaling have distinct kinetics. Initial MC signaling events such as PLCγ_1 phosphorylation and the release of Ca^{2+} from intracellular stores occur rapidly whilst PI3K-dependent signaling events are more delayed (Tkaczyk et al., 2003). This suggests that the delay may be due to a requirement for the store-dependent influx of extracellular Ca^{2+}, which in turn induces binding of CaM to t-FcεRIβ and translocation to the Golgi. Therefore it is likely that these events must take place before PI3K signaling can proceed.

We have demonstrated that t-FcεRIβ and Gab2 colocalized to the Golgi after MC activation and that the Golgi forms an intricate network with the MTOC. This therefore implicates involvement of the Golgi in microtubule formation and MC degranulation. Recent reports have suggested that the Golgi can not only regulate microtubule dynamics, but can also

initiate nucleation of microtubules (Hurtado et al., 2011; Rivero et al., 2009). The nucleation of microtubules initiated by the Golgi requires the interaction between the centrosome-associated protein AKAP450 and the *cis*-Golgi protein GM130 which are both required for the Golgi to form the pericentrosomal circular ribbon organization (Hurtado et al., 2011; Rivero et al., 2009) as was observed in this study. The interaction between AKAP450 and GM130 anchors the *cis*-Golgi to the centrosome and disruption of this interaction with truncated mutants of AKAP450 caused dissociation of the Golgi from the centrosome which negatively affected nucleation and secretion (Hurtado et al., 2011; Rivero et al., 2009). Thus the close association of t-FcεRIβ and Gab2 at the MTOC-Golgi interface may be key to t-FcεRIβ function.

It has been reported using EGFP-CaM chimeras, that CaM translocates to the MTOC after MC activation (Psatha et al., 2004). In addition, it has also been demonstrated that in T cells, Ras guanyl nucleotide releasing protein 1 (RasGRP1), an upstream activator of the PI3K pathway, translocates to the Golgi upon TCR activation where it activates Ras (Perez de Castro et al., 2004). Our observations are consistent with these reports as we propose that CaM binding to t-FcεRIβ is critical for this pathway. Also the phenotype of the t-FcεRIβ silenced cells closely resembles that of BMMC from RasGRP1$^{-/-}$ mice (Liu et al., 2007), suggesting a role for PI3K. BMMC from RasGRP1$^{-/-}$ mice display a significant reduction in both degranulation and cytokine production. In addition, there are defects in microtubule formation while F-actin rearrangement is not affected (Liu et al., 2007). We found that whilst F-actin dynamics were affected by silencing of t-FcεRIβ in human cells, mouse BMMC were unaffected and depolymerization of cortical F-actin, which has been shown to be driven by Ca^{2+} and Ca^{2+}-dependent kinases (Nishida et al., 2005), still occurred. Similarly to RasGRP1$^{-/-}$ BMMC, Fyn$^{-/-}$, Gab2$^{-/-}$ and PI3K$^{-/-}$ BMMC also display deficiencies in cytoskeletal dynamics and degranulation (Nishida et al., 2005; Suzuki et al., 2010), which suggests that t-FcεRIβ, Gab2 and RasGRP1 regulate a common PI3K pathway that ultimately forms the microtubular network required for granule translocation and degranulation.

This study has delineated a plausible mechanism behind a unique function for t-FcεRIβ, which may act to propagate Ca^{2+} signals linking Ca^{2+}-influx to microtubule nucleation and formation. We have demonstrated that t-FcεRIβ binds to Gab2 and kinases critical for microtubule formation, and that in the presence of Ca^{2+}, CaM binds to the t-FcεRIβ complex. This appears to be central to its function, possibly initiating phosphorylation and localization to the pericentrosome and Golgi. The potential roles of FcεRIβ in HuMC function are particularly important because the *MS4A2* gene is considered a candidate gene for the development of allergy and based upon the data presented in this manuscript, the gene product t-FcεRIβ is a plausible candidate. Thus the potential linkage of polymorphisms and/or mutations in t-FcεRIβ with allergy warrants further investigation. Furthermore, given the mechanism and binding partners of t-FcεRIβ, we predict that the t-FcεRIβ complex represents an excellent drug target for allergy and asthma, which would presumably be MC specific.

Experimental Procedures

Viral transduction of mast cells

For gene silencing in LAD-2 HuMC, MISSION® shRNA constructs and lentiviruses were used (Sigma-Aldrich, St Louis, MO) as described (Kuehn et al., 2010a). For constructs see (Supplemental material). For overexpression in HLMC, a custom-made Ad5C20Att01 virus containing the clone for FL-FcεRIβ (BioFocus DPI, Leiden, The Netherlands) was used as described (Cruse et al., 2010).

Immunoblotting

For details of antibodies used, see supplemental methods. For immunoblotting, LAD-2 HuMC were sensitized with 100 ng/ml biotinylated IgE overnight in LAD-2 medium without SCF (Kuehn et al., 2010b). Cells were then washed twice in HEPES buffer containing 0.04% BSA and resuspended at 2.5×10^6 cells/ml of HEPES buffer containing 0.04% BSA. The cells were challenged for 2 min with the indicated stimuli then immediately lyzed as described (Smrz et al., 2010). Immunoblots were carried out on the total cell lysates as described (Smrz et al., 2010). The acquired images were analyzed and densitometry was performed using ImageJ software (version 1.32).

Flow cytometry

To assay surface expression of FcεRIα and KIT, we used flow cytometric analysis on the FacsCalibur machine (BD Biosciences, San Jose, CA). Data were acquired with double staining for CD117 and FcεRIα. For some experiments, LAD-2 HuMC were transfected with GFP fusion constructs as described (Cruse et al., 2010).

Mediator release assays

For MC degranulation, β-hex was measured as described (Kuehn et al., 2010b). Histamine measurements were performed by radioenzymatic assay as described (Sanmugalingam et al., 2000). PGD_2-MOX (Cayman Chemicals, Ann Arbor, MI) and IL-8 (R&D Systems, Minneapolis, MN) were assayed as described (Kuehn et al., 2010b) and according to the manufacturer's instructions.

Measurement of intracellular Ca^{2+}

Changes in cytosolic Ca^{2+} levels were determined in SCF-deprived LAD-2 HuMC following loading of the cells with Fura-2 AM ester (Molecular Probes, Eugene, OR) as described (Tkaczyk et al., 2003). Fluorescence was measured at two excitation wavelengths (340 and 380 nm) and an emission wavelength of 510 nm. The ratio of the fluorescence readings was calculated following subtraction of the fluorescence of the cells that had not been loaded with Fura-2 AM.

Supplementary Material

Refer to Web version on PubMed Central for supplementary material.

Acknowledgments

Financial support was provided by the Division of Intramural Research of NIAID and NHLBI within the National Institutes of Health, and in part from an unrestricted pre-doctoral fellowship from Novartis Pharmaceuticals (GC). Work in Leicester was conducted in laboratories part-funded by ERDF #05567.

We thank the Biological Imaging Section, Research Technologies Branch, NIAID, NIH for expert advice in the acquisition and analysis of the confocal imaging. We also thank J. Rivera (NIAMS, NIH) for the generous gifts of FcεRIβ JRK Ab and *Ms4a2* KO mice.

References

Blank U, Rivera J. The ins and outs of IgE-dependent mast-cell exocytosis. Trends Immunol. 2004; 25:266–273. [PubMed: 15099567]

Cookson WO, Sharp PA, Faux JA, Hopkin JM. Linkage between immunoglobulin E responses underlying asthma and rhinitis and chromosome 11q. Lancet. 1989; 1:1292–1295. [PubMed: 2566826]

Cruse G, Kaur D, Leyland M, Bradding P. A novel FcεRIβ-chain truncation regulates human mast cell proliferation and survival. FASEB J. 2010; 24:4047–4057. [PubMed: 20554927]

Donnadieu E, Cookson WO, Jouvin MH, Kinet JP. Allergy-associated polymorphisms of the FcεRIβ subunit do not impact its two amplification functions. J Immunol. 2000a; 165:3917–3922. [PubMed: 11034399]

Donnadieu E, Jouvin MH, Kinet JP. A second amplifier function for the allergy-associated FcεRI-β subunit. Immunity. 2000b; 12:515–523. [PubMed: 10843384]

Draber P, Sulimenko V, Draberova E. Cytoskeleton in mast cell signaling. Front Immunol. 2012; 3:130. [PubMed: 22654883]

Funaba M, Ikeda T, Abe M. Degranulation in RBL-2H3 cells: regulation by calmodulin pathway. Cell Biol Int. 2003; 27:879–885. [PubMed: 14499669]

Furumoto Y, Nunomura S, Terada T, Rivera J, Ra C. The FcεRIβ immunoreceptor tyrosine-based activation motif exerts inhibitory control on MAPK and IκB kinase phosphorylation and mast cell cytokine production. J Biol Chem. 2004; 279:49177–49187. [PubMed: 15355979]

Gilfillan AM, Rivera J. The tyrosine kinase network regulating mast cell activation. Immunol Rev. 2009; 228:149–169. [PubMed: 19290926]

Gilfillan AM, Tkaczyk C. Integrated signalling pathways for mast-cell activation. Nat Rev Immunol. 2006; 6:218–230. [PubMed: 16470226]

Gimborn K, Lessmann E, Kuppig S, Krystal G, Huber M. SHIP down-regulates FcεR1-induced degranulation at supraoptimal IgE or antigen levels. J Immunol. 2005; 174:507–516. [PubMed: 15611277]

Hong H, Kitaura J, Xiao W, Horejsi V, Ra C, Lowell CA, Kawakami Y, Kawakami T. The Src family kinase Hck regulates mast cell activation by suppressing an inhibitory Src family kinase Lyn. Blood. 2007; 110:2511–2519. [PubMed: 17513616]

Hundley TR, Gilfillan AM, Tkaczyk C, Andrade MV, Metcalfe DD, Beaven MA. Kit and FcεRI mediate unique and convergent signals for release of inflammatory mediators from human mast cells. Blood. 2004; 104:2410–2417. [PubMed: 15217825]

Hurtado L, Caballero C, Gavilan MP, Cardenas J, Bornens M, Rios RM. Disconnecting the Golgi ribbon from the centrosome prevents directional cell migration and ciliogenesis. J Cell Biol. 2011; 193:917–933. [PubMed: 21606206]

Kashem SW, Subramanian H, Collington SJ, Magotti P, Lambris JD, Ali H. G protein coupled receptor specificity for C3a and compound 48/80-induced degranulation in human mast cells: Roles of Mas-related genes *MrgX1* and *MrgX2*. Eur J Pharmacol. 2011; 668:299–304. [PubMed: 21741965]

Kim SH, Bae JS, Holloway JW, Lee JT, Suh CH, Nahm DH, Park HS. A polymorphism of *MS4A2* (−109T > C) encoding the β-chain of the high-affinity immunoglobulin E receptor (FcεRIβ) is associated with a susceptibility to aspirin-intolerant asthma. Clin Exp Allergy. 2006; 36:877–883. [PubMed: 16839402]

Kinet JP. The high-affinity IgE receptor (FcεRI): from physiology to pathology. Annu Rev Immunol. 1999; 17:931–972. [PubMed: 10358778]

Kuehn HS, Jung MY, Beaven MA, Metcalfe DD, Gilfillan AM. Prostaglandin E2 activates and utilizes mTORC2 as a central signaling locus for the regulation of mast cell chemotaxis and mediator release. J Biol Chem. 2010a; 286:391–402. [PubMed: 20980255]

Kuehn HS, Radinger M, Gilfillan AM. Measuring mast cell mediator release. Curr Protoc Immunol. 2010b; Chapter 7(Unit 7):38. [PubMed: 21053305]

Laprise C, Boulet LP, Morissette J, Winstall E, Raymond V. Evidence for association and linkage between atopy, airway hyper-responsiveness, and the β subunit Glu237Gly variant of the high-affinity receptor for immunoglobulin E in the French-Canadian population. Immunogenetics. 2000; 51:695–702. [PubMed: 10941841]

Lin S, Cicala C, Scharenberg AM, Kinet JP. The FcεRIβ subunit functions as an amplifier of FcεRIγ-mediated cell activation signals. Cell. 1996; 85:985–995. [PubMed: 8674126]

Liu Y, Zhu M, Nishida K, Hirano T, Zhang W. An essential role for RasGRP1 in mast cell function and IgE-mediated allergic response. J Exp Med. 2007; 204:93–103. [PubMed: 17190838]

Lorentz A, Baumann A, Vitte J, Blank U. The SNARE Machinery in Mast Cell Secretion. Front Immunol. 2012; 3:143. [PubMed: 22679448]

Ma HT, Beaven MA. Regulators of Ca^{2+} signaling in mast cells: potential targets for treatment of mast cell-related diseases? Adv Exp Med Biol. 2011; 716:62–90. [PubMed: 21713652]

Nishida K, Yamasaki S, Hasegawa A, Iwamatsu A, Koseki H, Hirano T. Gab2, via PI-3K, regulates ARF1 in FcεRI-mediated granule translocation and mast cell degranulation. J Immunol. 2011; 187:932–941. [PubMed: 21653832]

Nishida K, Yamasaki S, Ito Y, Kabu K, Hattori K, Tezuka T, Nishizumi H, Kitamura D, Goitsuka R, Geha RS, et al. FcεRI-mediated mast cell degranulation requires calcium-independent microtubule-dependent translocation of granules to the plasma membrane. J Cell Biol. 2005; 170:115–126. [PubMed: 15998803]

Nishiyama C, Akizawa Y, Nishiyama M, Tokura T, Kawada H, Mitsuishi K, Hasegawa M, Ito T, Nakano N, Okamoto A, et al. Polymorphisms in the FcεRI β promoter region affecting transcription activity: a possible promoter-dependent mechanism for association between FcεRI β and atopy. J Immunol. 2004; 173:6458–6464. [PubMed: 15528387]

Parravicini V, Gadina M, Kovarova M, Odom S, Ganzalez-Espinosa C, Furumoto Y, Saitoh S, Samelson LE, O'Shea JJ, Rivera J. Fyn kinase initiates complementary signals required for IgE-dependent mast cell degranulation. Nat Immunol. 2002; 3:741–748. [PubMed: 12089510]

Perez de Castro I, Bivona TG, Philips MR, Pellicer A. Ras activation in Jurkat T cells following low-grade stimulation of the T-cell receptor is specific to N-Ras and occurs only on the Golgi apparatus. Mol Cell Biol. 2004; 24:3485–3496. [PubMed: 15060167]

Psatha M, Koffer A, Erent M, Moss SE, Bolsover S. Calmodulin spatial dynamics in RBL-2H3 mast cells. Cell Calcium. 2004; 36:51–59. [PubMed: 15126056]

Ra C, Jouvin MH, Kinet JP. Complete structure of the mouse mast cell receptor for IgE (FcεRI) and surface expression of chimeric receptors (rat-mouse-human) on transfected cells. J Biol Chem. 1989; 264:15323–15327. [PubMed: 2527850]

Rivera J, Gilfillan AM. Molecular regulation of mast cell activation. J Allergy Clin Immunol. 2006; 117:1214–1225. [PubMed: 16750977]

Rivero S, Cardenas J, Bornens M, Rios RM. Microtubule nucleation at the cis-side of the Golgi apparatus requires AKAP450 and GM130. EMBO J. 2009; 28:1016–1028. [PubMed: 19242490]

Sandford AJ, Shirakawa T, Moffatt MF, Daniels SE, Ra C, Faux JA, Young RP, Nakamura Y, Lathrop GM, Cookson WO, et al. Localisation of atopy and β subunit of high-affinity IgE receptor (FcεRI) on chromosome 11q. Lancet. 1993; 341:332–334. [PubMed: 8094113]

Sanmugalingam D, Wardlaw AJ, Bradding P. Adhesion of human lung mast cells to bronchial epithelium: evidence for a novel carbohydrate-mediated mechanism. J Leukoc Biol. 2000; 68:38–46. [PubMed: 10914488]

Shirakawa T, Li A, Dubowitz M, Dekker JW, Shaw AE, Faux JA, Ra C, Cookson WO, Hopkin JM. Association between atopy and variants of the β subunit of the high-affinity immunoglobulin E receptor. Nat Genet. 1994; 7:125–129. [PubMed: 7920628]

Singleton TE, Platzer B, Dehlink E, Fiebiger E. The first transmembrane region of the β-chain stabilizes the tetrameric FcεRI complex. Mol Immunol. 2009; 46:2333–2339. [PubMed: 19406478]

Smrz D, Iwaki S, McVicar DW, Metcalfe DD, Gilfillan AM. TLR-mediated signaling pathways circumvent the requirement for DAP12 in mast cells for the induction of inflammatory mediator release. Eur J Immunol. 2010

Suzuki R, Liu X, Olivera A, Aguiniga L, Yamashita Y, Blank U, Ambudkar I, Rivera J. Loss of TRPC1-mediated Ca^{2+} influx contributes to impaired degranulation in Fyn-deficient mouse bone marrow-derived mast cells. J Leukoc Biol. 2010; 88:863–875. [PubMed: 20571036]

Thastrup O, Cullen PJ, Drobak BK, Hanley MR, Dawson AP. Thapsigargin, a tumor promoter, discharges intracellular Ca^{2+} stores by specific inhibition of the endoplasmic reticulum $Ca^{2(+)}$-ATPase. Proc Natl Acad Sci U S A. 1990; 87:2466–2470. [PubMed: 2138778]

Tkaczyk C, Beaven MA, Brachman SM, Metcalfe DD, Gilfillan AM. The phospholipase $C_{\gamma 1}$-dependent pathway of FcεRI-mediated mast cell activation is regulated independently of phosphatidylinositol 3-kinase. J Biol Chem. 2003; 278:48474–48484. [PubMed: 13129935]

Vonakis BM, Chen H, Haleem-Smith H, Metzger H. The unique domain as the site on Lyn kinase for its constitutive association with the high affinity receptor for IgE. J Biol Chem. 1997; 272:24072–24080. [PubMed: 9295361]

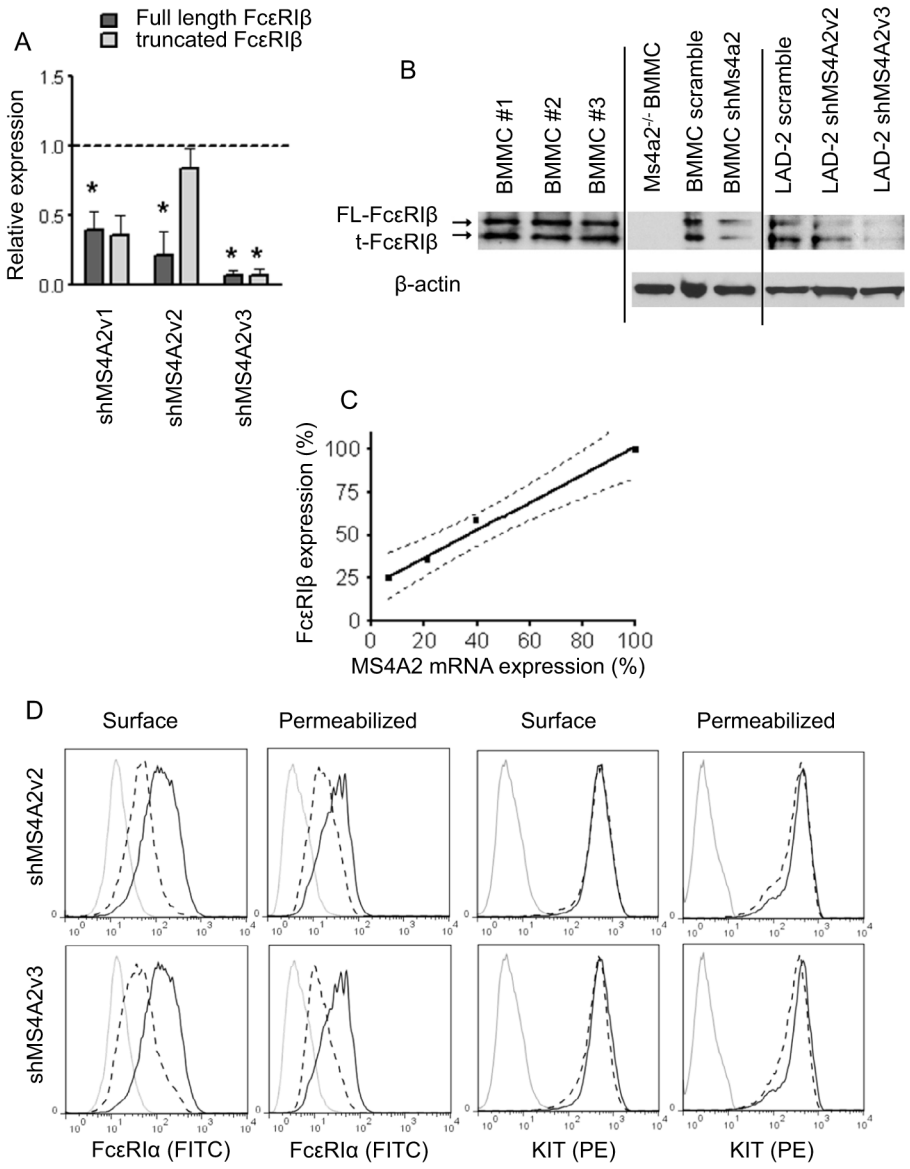

Figure 1. see also Figure S1

Validation of FcεRIβ silencing in LAD-2 HuMC. **A.** shMS4A2v1 silenced both FcεRIβ variants with low efficiency. shMS4A2v2 selectively silenced FL-FcεRIβ without accompanied silencing of t-FcεRIβ. shMS4A2v3 silenced both variants with high efficiency. Data are the means ± SEM (n=3). *p<0.05. **D.** Silencing the different constructs for FcεRIβ also resulted in a reduction in FcεRIβ protein levels. Two bands were detected in BMMC which corresponded to the predicted size of the FcεRIβ variants (~28 and ~22 kDa). These bands were not present in *Ms4a2*$^{-/-}$ BMMC. Data are representative of at least 2 separate blots. **E.** The reduction in FL-FcεRIβ mRNA expression correlates well with the reduction in FL-FcεRIβ protein levels. Each point represents the mean expression from the different shRNA constructs. $R^2 = 0.964$, p=0.018. **F.** Silencing of FL-FcεRIβ, shMS4A2v2 (top panels), and both FcεRIβ variants, shMS4A2v3 (bottom panels), reduced FcεRIα expression without affecting KIT expression. Both surface expression of FcεRIα and total expression of FcεRIα (permeabilized cells) significantly decreased following transduction.

Histograms are representative of at least 3 separate experiments. Gray line = isotype control, black line = scramble control, dashed line = shRNA constructs.

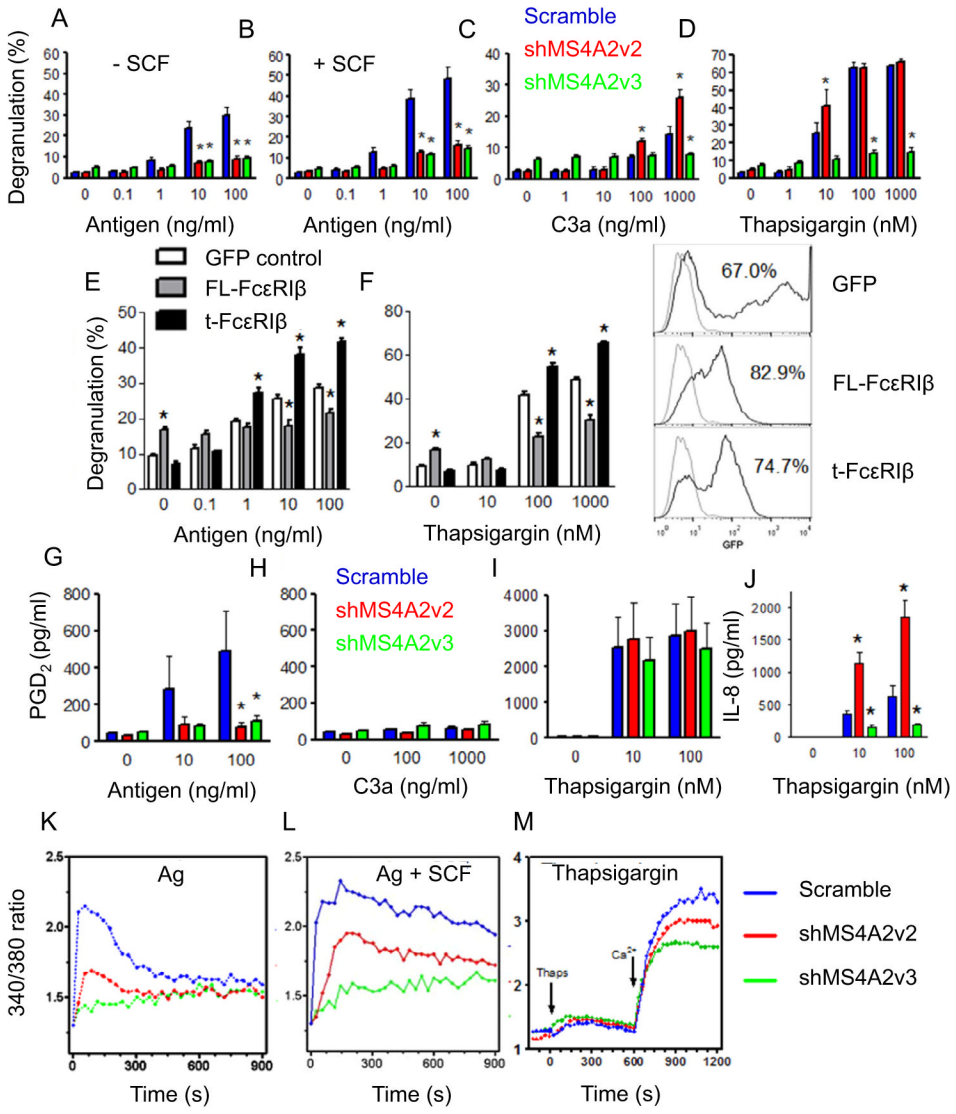

Figure 2. see also Figure S2

Multiple roles for FcεRIβ in MC degranulation. **A.** Both shMS4A2v2 and shMS4A2v3 inhibit antigen-induced β-hex release from LAD-2 HuMC to a similar degree. **B.** Addition of 100 ng/ml SCF increased β-hex release, but did not affect the degree of inhibition. **C.** IgE-independent degranulation induced by C3a was enhanced with FL-FcεRIβ targeting (shMS4A2v2 – gray bars) but was inhibited with silencing of both variants of FcεRIβ (shMS4A2v3 – open bars). **D.** Similarly, receptor-independent thapsigargin-induced β-hex release was potentiated with FL-FcεRIβ silencing at sub-maximal doses, but silencing both variants significantly reduced degranulation. Data are the means ± SEM from 4–6 experiments. *p<0.05. **E**. Overexpression of FL-FcεRIβ inhibits antigen-induced (**E**) and thapsigargin-induced (**F**) degranulation in LAD-2 HuMC whilst overexpression of t-FcεRIβ potentiates degranulation. Histograms demonstrate GFP expression assessed by FACS analysis prior to the assays. **G.** Both shMS4A2v2 and shMS4A2v3 inhibited antigen-induced PGD_2 release with similar efficacy to β-hex release. **H.** C3a did not induce PGD_2 release. **I.** Thapsigargin-induced PGD_2 release was not affected by either shMS4A2v2 or shMS4A2v3. **J.** IL-8 release induced by thapsigargin was potentiated with FL-FcεRIβ

silencing and significantly inhibited with shMS4A2v3. **K.** Ca^{2+} influx was reduced in antigen stimulated cells in the absence (**K**) and presence (**L**) of 100 ng/ml SCF which was comparable to mediator release. **M.** Ca^{2+} release from stores in response to thapsigargin was measured in Ca^{2+}-free medium and was unaffected either shRNA construct. Store-operated Ca^{2+} entry was then assessed by the addition of extracellular Ca^{2+} and modest reductions in Ca^{2+} influx with the shRNA constructs were observed. Data are the means ± SEM from 3 experiments (E–J) * $p<0.05$. Ca^{2+} imaging data are representative of 2 separate experiments performed in duplicate (K–M).

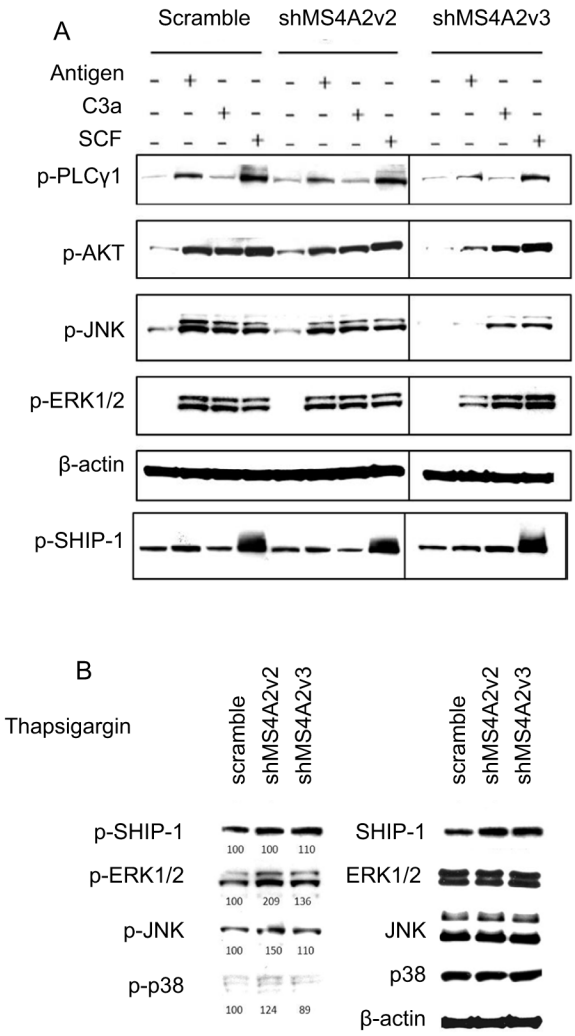

Figure 3. see also Figure S3

Effects of FcεRIβ silencing on LAD-2 HuMC signaling. **A.** LAD-2 HuMC were stimulated with either Ag (100 ng/ml), C3a (1000 ng/ml), SCF (100 ng/ml) or mock-treated for 2 min. Immunoblots demonstrating a small reduction in both PLCγ_1 and Akt phosphorylation with Ag stimulation with both shMS4A2v2 and shMS4A2v3. There were no significant differences with C3a and SCF stimulation. A similar pattern was observed with MAPK (Jnk and ERK1/2) phosphorylation. However, with the shMS4A2v3 cells, there was a reduction in Jnk phosphorylation with C3a and with SCF stimulation. There was no obvious difference in SHIP-1 phosphorylation with either shRNA construct. **B.** Immunoblots demonstrating that there was increased phosphorylation of MAPKs with shMS4A2v2, but there was no difference between the shMS4A2v3 and control after stimulation with 100 nM thapsigargin for 2 min. Numbers represent the relative phosphorylation compared to scramble control using densitometry with correction against total protein. Immunoblots are representative of at least 2 independent experiments.

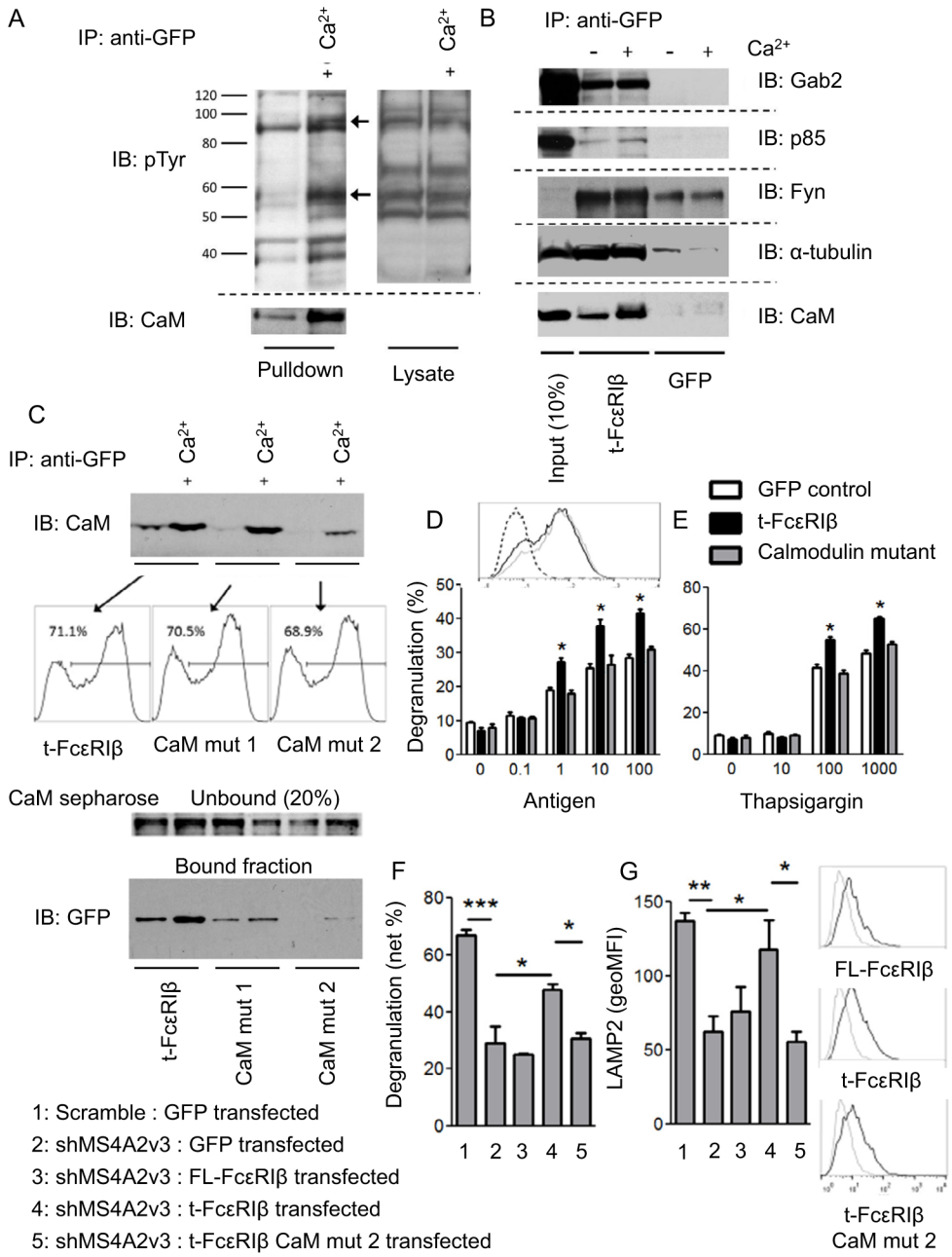

Figure 4. see also Figure S4

T-FcεRIβ coimmunoprecipitates with Gab2, α-tubulin, PI3K, Fyn kinase and binds calmodulin in the presence of Ca^{2+}. **A**. LAD-2 HuMC lysates were captured with an immunoprecipitated t-FcεRIβ:GFP chimera in the absence and presence of 2 mM Ca^{2+} and immunoblots demonstrated that CaM was pulled down preferentially with t-FcεRIβ in the presence of Ca^{2+}. Probing with a phosphotyrosine Ab demonstrated phosphorylated bands concentrated around 50–60 kDa (bottom arrow) and 80–100 kDa (top arrow) in the presence of Ca^{2+}. **B**. Immunoblotting for Gab2 (97 kDa), PI3K p85 (85 kDa), Fyn kinase (59 kDa) and α-tubulin (55 kDa) demonstrated pulldown of these proteins with t-FcεRIβ in the presence and absence of Ca^{2+}. Binding of CaM to the complex was again enhanced in the presence of Ca^{2+}. **C**. Mutation of the putative CaM binding domain of t-FcεRIβ reduced

CaM binding. This was particularly evident with CaM mut 2 (see text). Histograms demonstrate equal transfection efficiencies and level of expression for each construct prior to pull-downs. Similar results were obtained with immunoprecipitated GFP:t-FcεRIβ variants used as bait for CaM, and CaM sepharose beads used to pull out CaM-binding proteins from transfected lysates. Cell lysates, after pulldown, were run as the unbound fraction and were 5x less concentrated than the bound fraction. Immunoblots are representative of at least 2 independent experiments. **D.** Mutation of the CaM binding domain of t-FcεRIβ (CaM mut 2) eliminates the potentiation of degranulation from transfection of t-FcεRIβ into LAD-2 HuMC in response to both antigen (**D**) and thapsigargin (**E**). Inset: histogram demonstrating equal expression of t-FcεRIβ and CaM mut 2 measured by FACS analysis prior to assays for **D** and **E. F**. Transfection of WT t-FcεRIβ, but not t-FcεRIβ CaM mut 2, after silencing of both FcεRIβ isoforms partially recovered thapsigargin-induced degranulation measured by β-hex release (**F**) and surface LAMP2 (**G**). Inset: histograms demonstrate comparable expression levels for each transfected construct (gray = untransfected, black = transfected). Data are the means ± SEM from 3 experiments (**D**–**G**).*p≤0.05, **p≤0.01, ***p ≤0.001.

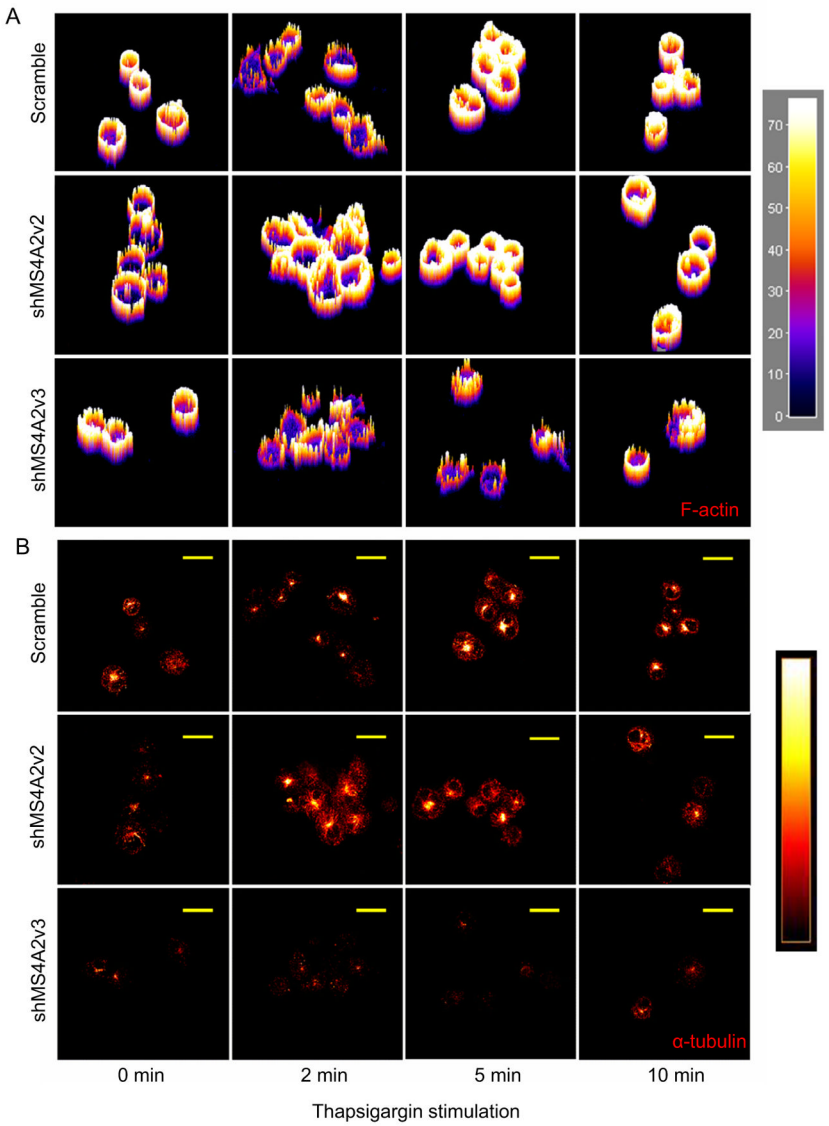

Figure 5. see also Figure S5

Silencing of t-FcεRIβ results in a deficiency in microtubule formation and cytoskeletal dynamics. **A**. 3D intensity plots demonstrating the dynamics of filamentous (F)-actin. The top panels demonstrate a decrease in fluorescence intensity of phalloidin (FITC) stained LAD-2 HuMC treated with scramble shRNA at 2 min post-stimulation with thapsigargin followed by a marked increase in intensity evident at 5 and 10 min. The middle panels and lower panels show the equivalent conditions with silencing of FL-FcεRIβ and both FL-FcεRIβ and t-FcεRIβ, respectively. There was a dramatic reduction in repolymerization of actin evident at 5 min when additional silencing of t-FcεRIβ (shMS4A2v3) was compared to scrambled control. **B**. Microtubule assembly. The top panels show the same cells as A co-stained for α-tubulin. There was a marked induction of microtubule formation with stimulation of the scramble control and FL-FcεRIβ silenced cells showing the typical intense point adjacent to the nucleus representing activation of the MTOC indicative of microtubule formation. Bottom panels show that there was a deficiency in microtubule formation with additional silencing of t-FcεRIβ. Data are representative of several fields

from 2 independent experiments. Yellow scale bar = 20 μm. Rabbit IgG control Ab was negative (see Figure S7).

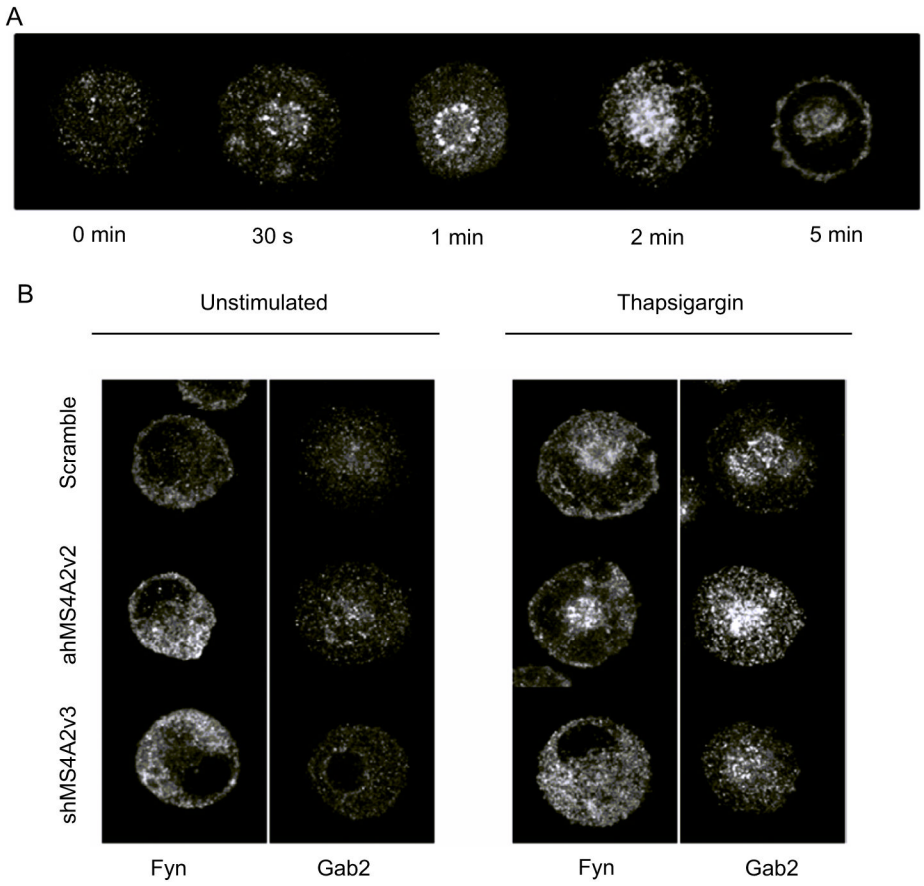

Figure 6. see also Figure S6 and Supplemental movie 1

The t-FcεRIβ complex translocates following Ca^{2+} influx. **A**. The t-FcεRIβ:GFP chimera transfected into LAD-2 HuMC rapidly translocates to form a ring-like structure adjacent to the nucleus after stimulation with 100 nM thapsigargin. **B**. Immunofluorescence and confocal micrographs of Fyn kinase and Gab2 localization following stimulation with 100 nM thapsigargin for 1 min. There was accumulation of both Fyn and Gab2 to a similar location as t-FcεRIβ after stimulation with thapsigargin in the scramble controls and with silencing of FL-FcεRIβ. However, when both variants of FcεRIβ were silenced perinuclear localization was less evident.

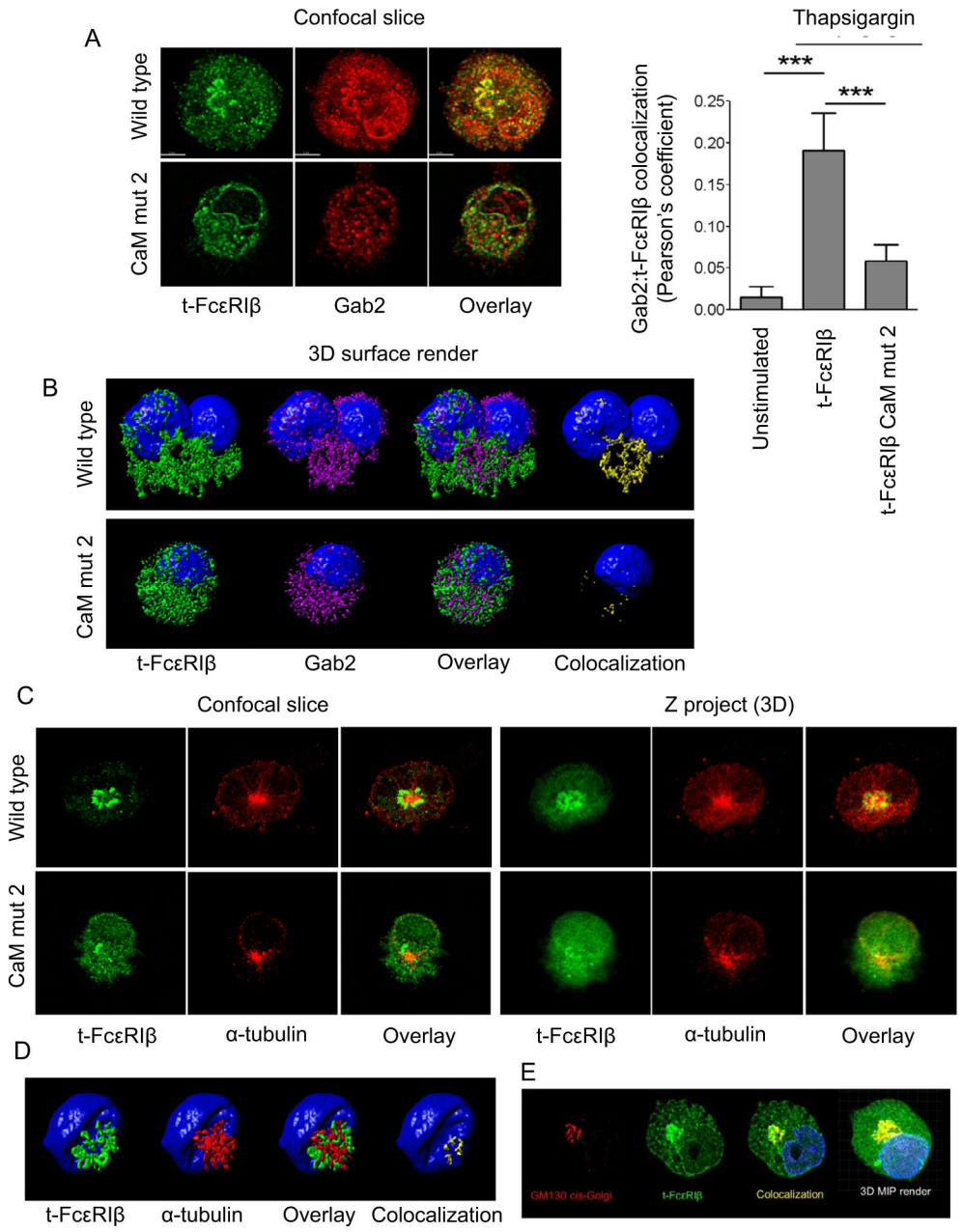

Figure 7. see also Figure S7 and Supplemental movies, 2, 3, 4 and 5

T-FcεRIβ and Gab2 colocalized to the Golgi Apparatus which surrounds the microtubule organization center. **A**. Confocal micrographs showing that t-FcεRIβ (green) and Gab2 (red) colocalized (yellow) to a structure near the nucleus (top panels). CaM mut 2 t-FcεRIβ exhibited reduced colocalization with Gab2 (bottom panels and bar graph – data expressed as mean ± SD, ***p<0.001 ANOVA). **B**. 3D reconstruction and surface rendering of deconvolved image stacks revealed t-FcεRIβ (green) and Gab2 (purple) form a structure with a hollow center adjacent to the bilobed nucleus (blue). There was colocalization (yellow) only in the region adjacent to the nucleus (top panels), which was less evident with CaM mut 2 (bottom panels). **C**. The t-FcεRIβ complex surrounds the MTOC. Confocal micrographs demonstrating that t-FcεRIβ (green) circles the MTOC, which appears as a

dense α-tubulin (red) rich region adjacent to the nucleus. 3D render of average intensity of the Z stack demonstrates that t-FcεRIβ surrounds the MTOC. The translocation of t-FcεRIβ was less evident with CaM mut 2 (bottom panels). **D**. 3D reconstruction of these structures revealed that the hollow center of the t-FcεRIβ (green) structure was completely filled with α-tubulin (red). There was little colocalization (yellow) of t-FcεRIβ and α-tubulin, but points of contact were apparent which could represent nucleation of microtubules at the Golgi. It was also apparent that the centrosome structure formed by the MTOC and t-FcεRIβ complex caused considerable indentation into the nucleus (blue). **E**. Confocal micrographs demonstrating that t-FcεRIβ (green) forms an identical structure as the *cis*-Golgi protein GM130 (red).